Effect of ultrasonic homogenization on the Vis/NIR bulk optical properties of milk

Ben Aernouts,[a*] Robbe Van Beers,[a] Rodrigo Watté,[a] Tjebbe Huybrechts,[a] Jeroen Jordens,[b] Daniel Vermeulen,[c] Tom Van Gerven,[b] Jeroen Lammertyn,[a] and Wouter Saeys[a]

[a]*KU Leuven, Department of Biosystems, MeBioS, Kasteelpark Arenberg 30, 3001 Leuven, Belgium*
[b]*KU Leuven, Department of Chemical Engineering, ProcESS, Willem de Croylaan 46, 3001 Leuven, Belgium*
[c]*KU Leuven, Department of Biosystems, Livestock-Nutrition-Quality, Kasteelpark Arenberg 30, 3001 Leuven, Belgium*
[*]Corresponding author: *Ben.Aernouts@kuleuven.be, +3216321470, KU Leuven, Department of Biosystems, MeBioS, Kasteelpark Arenberg 30, 3001 Leuven, Belgium*

Abstract

The size of colloidal particles in food products has a considerable impact on the product's physicochemical, functional and sensory characteristics. Measurement techniques to monitor the size of suspended particles could, therefore, help to further reduce the variability in production processes and promote the development of new food products with improved properties. Visible and near-infrared (Vis/NIR) spectroscopy is already widely used to measure the composition of agricultural and food products. However, this technology can also be consulted to acquire microstructure-related scattering properties of food products. In this study, the effect of the fat globule size on the Vis/NIR bulk scattering properties of milk was investigated. Variability in fat globule size distribution was created using ultrasonic homogenization of raw milk. Reduction of the fat globule size resulted in a higher wavelength-dependency of both the Vis/NIR bulk scattering coefficient and the scattering anisotropy factor. Moreover, the anisotropy factor and the bulk scattering coefficients for wavelengths above 600 nm were reduced and were dominated by Rayleigh scattering. Additionally, the bulk scattering properties could be well ($R^2 \geq 0.990$) estimated from measured particle size distributions by consulting an algorithm based on the Mie solution. Future research could aim at the inversion of this model to estimate the particle size distributions from Vis/NIR spectroscopic measurements.

Keywords

Food emulsion, Milk, Ultrasonic homogenization, Vis/NIR spectroscopy, Light scattering, fat globule size distribution

1. Introduction

Many products in the food industry, including milk, ice cream, mayonnaise, jam, etc., are colloids or have been produced via colloids. Dispersed particles determine, through their concentration, distribution, size and structure, the physicochemical and organoleptic quality properties of the product. Additionally, the complex interactions among colloidal particles and with other ingredients will contribute to the rheology, texture, stability, appearance, and many other food characteristics [1]. Techniques to measure the particle properties of the colloid systems allow for better understanding these complex relations and further improve food processing techniques and recipes. Furthermore, implementation of such sensing-technology in a food plant could enable online monitoring of the colloids or the derived products during the production process and promote early detection of an altering product quality [2].

Milk is a natural colloidal emulsion of fat globules, as well as a hydrocolloid suspension of casein micelles, both dispersed in a water-based solution [3]. The fat globules, with a size ranging from 0.1 to 15 μm, result from the assembly of small intracellular lipid droplets, followed by an apocrine secretion through the apical membrane of the epithelial cells in the mammary gland [4]. The volume fraction of these fat globules and casein micelles, the particle size and shape and particle-particle interactions contribute significantly to the quality

properties of dairy products [5]. Among these influential factors, the milk fat globule (MFG) size was found to have an important impact on the physicochemical, functional and sensory characteristics of the milk and derived products [5–9]. The size of the native fat globules is correlated with the fatty acid composition and bioavailability of the lipids [10–18]. Since the size of the globules, and more specifically the amount of fat globule membrane, has an impact on the enzymatic activity in the milk, it will affect the colloid stability. Furthermore, large fat globules cream faster and make skimming easier [13,19]. Centrifugation, gravity separation and microfiltration are methods to separate native MFGs of different sizes to create products with new, better and/or standardized properties [13,19–22]. High-pressure or ultrasonic homogenization can also reduce the size of the fat globules by disrupting them into smaller ones [23–28]. However, as the MFG membranes are disrupted too and casein micelles and whey proteins adsorb at the increased surface area, the properties for homogenized MFGs are different compared to small native MFGs [10,11,7,20]. Because of the impact of these techniques on the size of the fat globules and accordingly the food colloid properties, it is important to monitor these processes to ensure a high quality product with minimal intra- and inter-batch variability [6,29]. This is also the case for raw milk as there is a large variability in MFG quantity and size distribution, varying between milk of different cows, within individual cows between different milkings and quarters, and within individual quarter milkings between different times of sampling [6,29–31]. Hence, online prediction of the fat content and MFG size distribution, during the milking process, would allow for the separation of raw milk with different colloidal properties, depending on the needs of the food industry [32,33]. This could reduce the number of process steps in a food plant, promote the development of new food products with extra functional properties and upgrade the value of raw milk [29]. Additionally, as the size of MFG in milk from infected mammary glands is significantly increased, MFG size information obtained on the dairy farm could give insight into the udder health status of each individual cow and udder quarter [34,35].

Optical measurement techniques are frequently used to monitor processes in food industry and agriculture. Among them, spectroscopy studies the interaction between electromagnetic radiation (EMR) and the product of interest. Because of the relatively deep penetration, relaxing the requirements for sample preparation, visible (Vis) and near-infrared (NIR) spectroscopy is often preferred. It combines a fast and non-destructive measurement principle with robust and cost-efficient sensor technology available nowadays. Originally, Vis/NIR spectroscopy was used to study the wavelength-dependent absorption by molecules in the product. The measured absorption relates to the number of molecules that absorb at that wavelength and the sample thickness. Therefore, it can be consulted to predict the product's composition through the Beer-Lambert law. As most food and agricultural products contain local non-uniformities, the radiation is forced to deviate from its straight trajectory and the travelling path is increased to an unknown extent. These non-uniformities can be polymer, metal or mineral particles in industrial systems; fat globules in emulsions; cells, cell organelles, air pores and fibrous structures in biological tissues; or pores, air bubbles and crystals in processed foods, etc. These elastic scattering processes complicate the prediction of the composition from measured spectra as the measurements have to be corrected for this non-linear interference [32]. Moreover, samples with scattering properties that are out of the range compared to the samples used in the calibration will result in inferior predictions [36]. On the other hand, the scattering properties could also be exploited as a valuable source of information because the overall scattering level and the angular- and wavelength-dependency are determined by the physical microstructure of the product. For emulsions, the scattering properties are related to the quantity, size distribution and material properties (refractive index) of the suspended spherical particles [6,23–26,37].

In the last decade, several models and measurement techniques based on Vis/NIR spectroscopy have been proposed to quantify the absorption and scattering properties for homogeneous food products [38–42]. The derived bulk absorption coefficient μ_a (cm^{-1}) is defined as the probability of absorption per unit infinitesimal path length and can be related to the product composition without the need for (empirical) scatter corrections. The scattering,

on the other hand, can be described with the bulk scattering coefficient μ_s (cm^{-1}) and the angular scattering pattern: the normalized scattering phase function $p(\theta)$. μ_s describes the probability of scattering per unit infinitesimal path length, analogous to μ_a, while $p(\theta)$ gives a detailed description of the normalized scattering probability as a function of the scattering angle θ. As $p(\theta)$ is often too complex to represent and interpret, only the first moment of $p(\theta)$, defined as the scattering anisotropy factor g, will generally be considered and represents the mean cosine of the scattering angle. The anisotropy factor for biological tissues and emulsions in the Vis/NIR range varies between isotropic Rayleigh scattering ($g = 0$) and complete forward scattering ($g = 1$) [43]. Extraction of these bulk scattering properties from Vis/NIR spectroscopic measurements, and prediction of the particle size distribution (PSD) of the measured emulsion from these properties could create a whole new field of applications for Vis/NIR spectroscopy. As Vis/NIR spectrometers are already well established for compositional analysis in the agro-food industry, extending their functionalities with PSD estimations would further promote the implementation of this technology [6,44].

In order to derive microstructure information (e.g. PSD) from measured bulk scattering properties (μ_s and $p(\theta)$), the complex relation between those two has to be unravelled by solving Maxwell's equations for electromagnetic theory [43]. Since the scattering particles in an emulsion are almost perfectly spherical, the equations can be evaluated with the Mie solution. The Mie solution for Maxwell's equations describes the electromagnetic field inside and outside a spherical scatterer for given particle properties. Nowadays, algorithms that rely on the Mie solution are available to simulate the bulk optical properties (μ_a, μ_s and $p(\theta)$ or g) for polydisperse spherical particles in an absorbing host medium, taking into account the particle's volume concentration and size distribution, the complex refractive indices of particle and medium, and the considered radiation wavelength [37,45]. Consequently, inversion of these algorithms would clear the way for PSD estimations from measured bulk scattering properties [6].

However, these algorithms build on a number of assumptions which may not always be valid for food colloid systems. Apart from the assumption of perfect sphericity of the particles, these algorithms also assume that scattering events are independent. Under this condition, μ_s follows a linear increase (through the origin) with increasing particle quantity, while the normalized scattering phase function and the anisotropy factor are independent. In practice, however, the independent scattering relation becomes invalid when the particle volume concentration is above a certain threshold. It has been shown that this limit depends on the radiation wavelength, refractive indices of the particles and host medium and the particle size, shape and polydispersity [46,47]. Beyond this limit, scattering particles are close enough such that individual scattering events can influence each other. This dependent scattering typically reduces the bulk scattering coefficient and the anisotropy factor compared to what could be expected from the independent scattering relations [48–50].

To evaluate the concept of PSD estimation from the bulk scattering properties of milk, it is crucial to validate the accuracy and robustness of the algorithms that relate the bulk scattering properties to the particle size distribution of milk. Accordingly, this is the main objective of the present study. More specifically, the effect of the fat globule size and quantity on the bulk optical properties (BOP) of milk was investigated by measuring milk samples with the 'golden standard' method and comparing them to the BOP simulated from the measured particle size distributions.

This manuscript is an extended and improved version of a conference proceeding presenting the preliminary results [40]. Moreover, the PSD measurements were measured with a laser diffraction apparatus with improved sensitivity for submicron particles (paragraph 2.2), while the accuracy of the unscattered transmittance measurements was further enhanced (paragraph 2.3).

2. Materials and methods

2.1 Milk samples and ultrasonic homogenization of milk

A fresh, raw bulk milk sample was collected from a Belgian dairy farm. The major components were measured with a Milkoscan FT+ (Foss A/S, Hillerød, Denmark) milk analyzer according to ISO 9622:2000. The fat, crude protein, lactose and water content were respectively 4.12%, 3.53%, 4.55% and 89.7% (all *w*/*v*). To create milk samples with different PSDs, the original raw milk sample was heated up to 37 ± 1°C in a water bath, gently shaken and split into 7 subsamples of 20 ml (polypropylene cup, 28 mm diameter and 68 mm high) to be homogenized with ultrasound for respectively 0 (raw), 20, 60, 120, 300, 600 and 1200 s. Ultrasound waves were generated by a Vibra-Cell VCX400 (400 Watt, 20kHz) equipped with a CV26 converter, a standard 13 mm horn and a tapered 3 mm microtip (all Sonics & Materials Inc., Danbury, USA). The microtip was immersed into the milk at a depth of 5 ± 1 mm. The power level of the ultrasound generator was fixed at 20% (80 Watt) to prevent the milk from foaming, but still maintaining a high homogenization efficiency. During homogenization, the cup with the milk sample was cooled in a water bath at ±24°C to maintain a constant sample temperature of 37 ± 1°C. Consequently, denaturation of the proteins was prevented and a high homogenization efficiency was preserved [27]. For additional comparison, a commercial half-skimmed, homogenized (further referred to as 'Skim') milk sample (Joyvalle, Belgium), with a fat and crude protein content of respectively 1.5% and 3.5% (both *w*/*w*), was also considered in this study.

The PSDs and bulk optical properties (BOP) were measured for all 8 samples (next paragraphs). To test the validity of the independent scattering condition, the BOP of the raw milk sample and the milk samples homogenized for 120 and 1200 s were, next to their pure state ($^1/_1$), also measured after two- ($^1/_2$) and three-fold dilution ($^1/_3$) with deionized water.

2.2 Milk particle size distribution measurements with laser diffraction

The size distribution of fat globules in raw and homogenized milk is generally measured with laser diffraction (LD) after dissociating the suspended casein micelles [10,11,14–16,18,7–9,20,28,29,51–62]. Nevertheless, studies showed that the presence of casein micelles does not interfere with the size distribution of the fat globule fraction as determined with LD [28,59,62]. Moreover, the protein dissociating additives might also affect the actual fat globules as they can disrupt the MFG membrane proteins [59]. Therefore, the fat globule size distribution can be determined through LD without the need for casein micelle dissociation [13,6,63,64]. This is especially true for raw milk as there is (nearly) no overlap in the fat globule and casein micelle size.

The size distribution of milk casein micelles is usually determined with dynamic light scattering (DLS) after removing the fat globules through skimming [65–74]. However, the particle size measured with DLS relates to the hydrodynamic radius of the dynamic hydrated/solvated particle. The latter depends, next to the actual particle radius, also on the interaction between the particles and the solvent. As the surface of the casein micelles is covered with highly hydrophilic layer of κ-casein, the hydrodynamic radius is significantly larger than the particle-core radius [67]. In this study, however, the particle-core size is of interest as this one relates to the static light scattering and consequently the BOP of the suspension. In contrast, the PSD measured with LD techniques is related to the actual particle-core size. Further on, the newest generation LD devices are sufficiently accurate to also measure the size of sub-micron colloidal particles as small as 10 nm [75,76]. As a result, LD is used in numerous recent studies to determine the size of casein micelles in skimmed milk [56,60,77–85]. In these studies, the fat globules were removed from the milk through centrifugation or microfiltration in order to measure the PSD of only the casein micelle fraction. Nevertheless, the measured PSD of the casein micelle fraction, as determined with LD techniques, was found to be nearly independent of the presence of fat globules [56,59,60,84]. Additionally, the centrifugation and/or microfiltration process step might affect

the actual casein micelles size distribution. Consequently, it was concluded that the casein micelle size distribution can be determined through LD without removal of the fat globules, especially in raw milk [56,59,60,84].

In this study, the size distribution of the fat globules and casein micelles was measured simultaneously with LD. The Hydro EV sample dispersion unit of the LD equipment (Mastersizer 3000, Malvern, UK) was filled with 600 ml of deionized water and the stirring speed was set at 2400 rpm. Milk was added drop-wise until the red laser (633 nm) obscuration due to light scattering was 7±1% (ISO 13320:2009). Measurements were obtained directly after reaching the intended obscuration level as casein micelles start to break down due to low calcium concentrations at high dilution ratios [86]. Each sample was loaded two times to the LD instrument and 5 measurements were obtained per loading. The PSD of the fat globules and casein micelles was estimated from the measured angular scattering intensities by fitting the Mie model for spherical particles (Mastersizer 3000 software, Malvern, UK). The Mie model uses the refractive indices for the milk particles and milk serum at the wavelengths of the instrument's light sources, respectively 633 (red) and 470 nm (blue) [57,87]. Next, the goodness of fit was evaluated based on the residual and the weighted residual. According to ISO 13320:2009, a weighted residual above 1% might indicate an erroneous measurement and/or the use of incorrect refractive indices for the sample and dispersant. In this study, only PSD's were considered if the residual and the weighted residual of the fit were below respectively 0.8% and 0.6%. Next, the repeatability of the measurement and fitting procedure was evaluated based on the coefficient of variation (CV) for the Dv10, Dv50 and Dv90, being the particle diameter for which respectively 10, 50 and 90% (*v*/*v*) of the particles is smaller than or equal to (ISO 13320:2009). Only if the CVs for the Dv10, Dv50 and Dv90 were below 2% for all 10 (2 x 5) measurements on a sample, the average PSD was calculated and considered in the further analysis.

The PSD of casein micelle fraction and fat globule fraction could clearly be separated for raw milk, but were overlapping if fat globules were disrupted due to homogenization. The PSD of the casein micelles itself could be determined from the first mode (< 0.8 µm diameter) of the bimodal PSD of the raw milk sample. It was assumed that the casein micelle volume fraction and size distribution were not influenced by the ultrasonic homogenization process. Accordingly, the fat globules size distributions for all 8 milk samples could be obtained from the originally measured PSDs after subtracting the casein micelle size distribution.

Additionally, the fat globules for the raw milk sample and the milk samples homogenized for 120 and 1200 s were also inspected with a Leitz Diaplan microscope (Leica Microsystems GmbH, Wetzlar, Germany) at 1250x magnification.

2.3 Measurement of bulk optical properties for raw and homogenized milk samples

Double integrating sphere (DIS) and unscattered transmittance measurements are considered to be the 'golden standard' to determine the BOP (μ_a, μ_s and g) for thin samples of turbid media and were therefore used in this study [88]. The diffuse reflectance and total transmittance were measured simultaneously on the milk sample loaded in a borosilicate cuvette with a path length of 600 µm and positioned between the two integrating spheres, both equipped with a Vis and NIR detector. The unscattered transmittance was measured in a separate path with the Vis and NIR detector positioned 1.5 m behind the sample, which was loaded in a similar cuvette with a path length of 170 µm. A series of slits between sample and detector further reduced the number of scattered photons captured in the unscattered transmittance signal [48,88]. The sample illumination was especially designed to obtain high signal-to-noise spectra in the 500 – 2250 nm wavelength range for very turbid media. It consists of a supercontinuum laser light source (500 – 2250 nm, 4 Watt optical power) in combination with a high-precision monochromator. For more details on the measurement principle, the setup, its validation and the calibration and measurement procedure, the reader is referred to [88]. All sample spectra were measured from 500 until 1900 nm in steps of 10 nm by automated scanning of the monochromator. The samples were thoroughly stirred before they were measured at room temperature.

The inverse adding doubling (IAD) routine developed and optimized by Prahl [89] was consulted to obtain the BOP values from the diffuse reflectance and total and unscattered transmittance measurements. Apart from the three measurements, also the real refractive index of the sample had to be provided to the algorithm and was calculated with the equation proposed in [87]. Because of significant contribution of scattered photons to the unscattered transmittance signals, no BOP estimation could be established for raw milk at wavelengths below 600 nm and for milk samples homogenized for 20, 60, 120 and 300 s at wavelengths below 550 nm [48,88].

2.4 Simulation of the bulk optical properties for raw and homogenized milk samples

The BOP of the commercial, raw and homogenized milk samples were also calculated from their respective PSD with an algorithm to simulate the BOP of polydisperse suspensions of spherical particles in an absorbing host medium [45]. In this algorithm, the Mie solution for Maxwell's equations has been generalized to account for the effect of an absorbing host medium on the particle's scattering properties. Polydispersity of the particle system is supported by fractionalization of the provided PSD, while the number of intervals is automatically optimized in an efficient iterative procedure. This procedure is straightforward as it does not involve an inversion or fitting procedure. For more details on the algorithm and its validation, the reader is referred to [45]. In this study, the algorithm was used to simulate the BOP of the samples in the 500 – 1900 nm wavelength range, starting from the measured PSDs and refractive indices obtained from literature.

The BOP for the fat globule fraction and casein micelle fraction were simulated separately as their refractive indices differ significantly. Moreover, the fat globule size distribution, fat volume concentration and fat and milk serum refractive indices were provided as inputs for the algorithm to simulate the BOP for the fat globule fraction, while a similar approach was followed for the casein fraction. The fat volume concentration was found to be 4.52% *v*/*v*, as derived from the fat content (paragraph 2.1) and the fat and milk density of respectively 0.912 and 1.03 g/ml [87]. The casein volume concentration was 2.00% *v*/*v*, calculated from the crude protein content (paragraph 2.1), by taking into account the average casein fraction in crude protein (75.5% *w*/*w*) and the density of casein (1.33 g/ml) and milk [87]. The real part of the refractive index spectra for milk fat, casein and milk serum was obtained by adding a baseline to the Vis/NIR refractive index spectrum of water [90]. The baseline was determined at 589 nm, a wavelength for which the refractive indices are known for water, milk fat, casein and milk serum [87,90]. The imaginary part of the refractive index for milk fat, casein and milk serum was calculated from the bulk absorption coefficients of respectively fat, protein and a mixture of water, lactose and serum proteins [37,90–93]. The calculated BOP for the fraction of fat globules and casein micelles were afterwards recombined, similar to the recombination of different PSD fractions, to obtain the BOP of the milk samples [45].

3. Results and discussion

3.1 Particle size distribution of raw and homogenized milk samples

PSDs were considered after they passed the quality inspections given in paragraph 2.2. The final cumulative volume-frequency PSD for each of the 8 milk samples was calculated as the average of the passed replicates and is presented for each sample in Fig. 1. For raw milk, an explicit bimodal PSD can be noticed. Casein micelles with a size between 0.01 and 0.8 µm and fat globules with a size between 0.8 and 12 µm represent respectively the first and second mode. As the homogenization time increases, fat globule size is reduced, resulting in an overlap with the casein micelles. For the commercial milk sample and for samples homogenized over a period of 300 s and longer, no distinction in size can be made between the casein micelles and fat globules.

The casein micelle size distribution, derived from the first mode of the bimodal PSD for raw milk, was subtracted from all the measured PSDs, resulting in the cumulative volume-frequency size distribution for the fat globules [Fig. 2]. This subtraction method resulted in smooth monomodal PSDs, which indicates that the ultrasonic homogenization process had no noticeable effect on the casein micelle volume fraction and size distribution [94], as was assumed earlier (paragraph 2.2). Fig. 2 clearly demonstrates that the size of the fat globules decreases with increasing homogenization time, which implicates that their quantity increases. The PSD derived for the casein fraction is also presented in Fig. 2.

The most important properties describing the PSDs in Fig. 1 and Fig. 2 are listed in Table 1. Next to the percentiles Dv10, Dv50 and Dv90, also the surface area moment mean (D32) and the volume moment mean diameter of the particles (D43) are presented. Before subtraction of the casein micelle PSD [Table 1(a)], homogenization had nearly no effect on the Dv10 as the 10% (*v*/*v*) smallest particles were mainly casein micelles. All other PSD properties reduced steadily with increasing homogenization time. The half-skimmed (Skim) milk sample contained fat globules of similar size compared to the milk sample homogenized for 1200 s. However, the PSD width for the '1200 s' sample is wider [Table 1(b) and Fig. 2].

In respectively Fig. 3, Fig. 4 and Fig. 5, the microscopic images (1250x magnification) of raw milk and milk homogenized for 120 and 1200 s are illustrated. They clearly demonstrate the effect of ultrasonic homogenization on the size of the fat globules. After 1200 s of ultrasonic homogenization, the fat globules are too small to be clearly noticeable with an optical microscope.

3.2 Measurement of the bulk optical properties for raw and homogenized milk samples

The BOP for the 8 undiluted milk samples were obtained through IAD from DIS and unscattered transmittance measurements. For all the raw and homogenized milk samples, the measured bulk absorption coefficient spectra were very close ($R^2 \geq 0.968$) to each other and to the μ_a spectrum of the water fraction (89.7% *v*/*v*) [90]. This is because the composition of these samples is exactly the same, and water is by far the most important Vis/NIR absorbing milk component [Fig. 6]. In respectively Fig. 7 and Fig. 8, the measured bulk scattering coefficient spectra (μ_s) and scattering anisotropy spectra (g) are illustrated for the undiluted milk samples. Both the μ_s spectra [Fig. 7] and the g spectra [Fig. 8] are highly susceptible to the size (distribution) of the scattering fat particles. Ultrasonic homogenization for less than one minute resulted in an increase of the μ_s for radiation wavelengths below 600 nm and a decrease of the μ_s at longer wavelengths, while longer homogenization induced an overall decrease of the sample's Vis/NIR μ_s spectrum. Furthermore, with reducing particle size, the μ_s spectra became more dependent on the radiation wavelength (λ), approaching Rayleigh scattering ($\sim\lambda^{-4}$) [43]. The μ_s spectrum for the half-skimmed milk sample was lower compared to the '1200 s' sample, despite the similar fat globule size. This can mainly be explained by the lower fat volume concentration and consequently a lower quantity of scattering fat globules [23–26].

The anisotropy factor for the raw milk sample in the Vis/NIR range was relatively high (0.934 – 0.960) and nearly independent of the radiation wavelength. With reducing fat globule size, the anisotropy factor decreased and became more wavelength-dependent. This reduction in g indicates that the light scattering was more isotopic, which is typical for smaller scattering particles [43]. No accurate values for the anisotropy factor could be established for the samples 'Skim' and '1200 s' for radiation wavelengths above 1000 and 1450 nm, respectively. This was caused by diffuse reflectance values close to the noise level due to the very high absorption by water ($\geq$ 89.7% *v*/*v*) in combination with low scattering ($\mu_s < 10$ cm^{-1}). If scattering processes are independent of each other, the g spectrum should be independent of the particle quantity [48]. However, despite their similar fat globule size and similar casein micelle size [Table 1(b)], the g spectrum for the half-skimmed milk sample was lower compared to the '1200 s' sample. Because the fat globule quantity was lower in sample 'Skim', while the casein micelle quantity was similar, the micelles would have contributed more to the final g spectrum of sample 'Skim' compared to '1200 s'. As the casein micelles

were smaller than the fat globules [Table 1(b) and Fig. 2], this resulted in a lower *g* spectrum and more isotropic scattering [Fig. 11]. Consequently, the *g* spectrum for sample 'Skim' was lower.

3.3 Effect of dependent scattering on the bulk scattering coefficient in raw and homogenized milk samples

To test the validity of the independent scattering condition, the BOP for the raw milk sample and the milk samples homogenized for 120 and 1200 s were, next to their pure state ($^1/_1$), also measured after a two-fold ($^1/_2$) and three-fold ($^1/_3$) dilution with deionized water. The concentration of scattering particles in the pure, two-fold and three-fold diluted samples was respectively 6.52%, 3.26% and 2.17% (*v*/*v*). No consistent differences between the *g* spectra for the 3 particle concentrations could be detected for any of the 3 samples (results not shown). This is probably because the noise on the measured *g* spectra was more significant than the differences caused by the effect of dependent scattering at these particle volume concentrations. It is well known that an anisotropy factor derived from DIS and unscattered transmittance measurements is more prone to measurement noise in comparison to the other derived BOPs [88]. Moreover, the effect of dependent scattering on the anisotropy factor is only significant for relatively high volume concentrations of the scattering particles [48].

In Fig. 9, the measured μ_s spectra for the 3 samples (Raw, 120 s and 1200 s) and the 3 considered particle concentrations ($^1/_1$, $^1/_2$ and $^1/_3$) are shown. The μ_s spectra for the '$^1/_2$' and '$^1/_3$' samples were multiplied with respectively 2 and 3 to scale them all to the same particle concentration according to the linear independent scattering relation. Consequently, the differences between the scaled μ_s spectra for the same sample are caused by dependent scattering. For all samples, the highest volume concentration of scattering particles (pure sample) clearly produced lower μ_s spectra as could be expected from the linear independent scattering relation [Fig. 9]. Moreover, this effect was, to a smaller extent, still present in the μ_s spectra for the two-fold dilution of the homogenized samples. For the raw milk sample, no differences (R^2 = 0.999) were found between the scaled μ_s spectra for the '$^1/_2$' and '$^1/_3$' samples. This indicates that the independent scattering relation is valid up till higher particle volume concentrations if the scattering particles are larger and confirms the observations reported by other researchers [48,88,95–99]. Therefore, in raw milk samples, independent scattering is valid up to particle volume concentrations of at least 3.26% (two-fold dilution). For the homogenized samples, the difference between the scaled μ_s spectra for the '$^1/_2$' and '$^1/_3$' samples is very small. Therefore, dependent scattering is likely absent in homogenized milk samples with particle volume concentrations up to 2.17% (three-fold dilution).

3.4 Simulation of the bulk optical properties in raw and homogenized milk samples

As dependent scattering was present in the pure milk samples and in most of the two-fold diluted samples [Fig. 9], while the simulation algorithm assumes independent scattering, the BOP were simulated and validated for the three-fold diluted samples. The BOP were simulated separately for the casein micelle fraction and fat globules, and were recombined afterwards to obtain the BOP of the milk samples. The simulated bulk absorption coefficient spectra matched well ($R^2 \geq 0.973$) with the measured ones. These spectra are, however, not shown here as there was no visible difference between them and the μ_a spectrum of their water fraction (96.6% *v*/*v* for three-fold diluted milk) [90]. The simulated and measured spectra for respectively the bulk scattering coefficient spectra (μ_s) and scattering anisotropy spectra (*g*) are shown in Fig. 10 and Fig. 11. As illustrated in these figures and Table 2, the agreement between the simulated and measured bulk scattering properties for the three-fold diluted samples is very good. The poorest agreement (R^2 = 0.777) was found between the simulated and measured *g* spectra for the raw milk sample. As the anisotropy factor for raw milk is nearly independent of the radiation wavelength, the very small disagreement (RMSD = 2.33×10^{-3}) already resulted in a rather poor R^2. Comparison between all other simulated and measured bulk scattering properties resulted in an R^2 above 0.94. For all three samples together (raw, 120 s and 1200 s), the correlation between the simulated and measured

properties was very high, indicated by the very high coefficients of determination (respectively 0.990 and 0.996) for the bulk scattering coefficients and the anisotropy factors [Table 2]. The effect of homogenization on the measured and simulated bulk scattering properties is fairly the same. This indicates the high potential of the Mie solution, after inversion, to accurately estimate the PSD from BOP measurements. The high correlation between simulated and measured bulk optical properties indicates a successful triple validation of (1) the PSD measurements, (2) the BOP measurements and (3) the simulation algorithm. Small differences between the simulated and measured values in Fig. 10 and Fig. 11 could be due to errors in the measurement of the BOP and/or PSDs and/or because of invalidity of the perfect sphericity and independent scattering assumptions. However, they are more likely the result of incorrect simulation-inputs for the refractive indices. Therefore, accurate measurement of the complex refractive indices for milk fat, casein and milk serum for the entire Vis/NIR wavelength range could enable more accurate simulations.

In contrast to the preliminary results presented in [40], the present manuscript shows a much better agreement between simulated and measured BOP. Likely, this is the result of optimized unscattered transmittance measurements and improved sensitivity for submicron particles in the PSD measurements.

The simulated bulk scattering coefficient spectrum and scattering anisotropy spectrum for the 'virtual' casein fraction are also shown in respectively Fig. 10 and Fig. 11. As the casein micelles are relatively small [Table 1(b)], the g spectrum is low and is strongly dependent on the radiation wavelength. Moreover, in combination with a low volume concentration of casein, relative to the fat fraction (paragraph 2.4), this results in a very low μ_s spectrum, with nearly no scattering in the NIR. As a consequence, the μ_s spectrum for the casein micelles will not contribute much to the μ_s spectra of the milk samples. Likewise, also the simulated g spectrum for the casein micelles will have no substantial impact on the g spectra of the raw and homogenized milk samples.

Casein micelles are, however, not perfectly spherical, but a nearly-spherical cluster of smaller casein sub-micelles [5]. For non-spherical particles, the simulated μ_a and μ_s for equivalent spheres will be sufficiently accurate. However, the anisotropy factor g and scattering phase function $p(\theta)$ can differ significantly [37]. For this reason, the simulated g spectrum for the casein micelles in Fig. 11 might not be entirely correct. The T-matrix method for sphere clusters could be a good alternative for the Mie solution [100–102]. However, as it introduces extra degrees of freedom, it might import additional sources of error and should, therefore, be validated thoroughly. As the fat globules dominate the bulk scattering properties of milk, it is difficult to study the BOP of the casein micelles separately. Therefore, isolation of the casein micelles without damaging and without loss of micelles is essential in order to measure their exact BOP and validate the simulated results.

To enable online PSD measurements on turbid colloids with a particle volume concentration above 2 – 4%, dilution is not preferred to reduce dependent scattering. Therefore, a model is needed that describes the effect of dependent scattering on the bulk scattering properties. Recently, the Percus-Yevick model for dependent scattering was proposed and successfully validated on colloidal suspensions [49,50,103,104]. Moreover, studies on milk showed that this model is accurate for total volume fraction of fat globules and/or casein micelles up to 45% [49,50]. Further exploration of this model is, however, needed to evaluate the influence of the radiation wavelength, particle and host refractive indices and particle geometry, size, polydispersity and density [23,25].

Online measurement of the BOP for an undiluted colloidal suspension is possible with time- or spatially-resolved Vis/NIR spectroscopy [38–42]. With the development of a general model that describes dependent scattering, measured bulk scattering properties could be transformed to follow the independent scattering relation. Consequently, after inversion of the Mie solution, the transformed bulk scattering properties could be consulted to predict the PSD of the suspended particles [105].

4. Conclusions

Ultrasonic homogenization of milk reduces the size of its fat globules in relation to the exposure time. As a result, the bulk scattering properties change significantly and can, therefore, be consulted to extract size distribution information. With decreasing diameter of the fat globules, the visible (Vis) and near-infrared (NIR) bulk scattering coefficient and scattering anisotropy factor reduce and become more dependent on the radiation wavelength.

In absence of dependent scattering, the Mie solution can accurately ($R^2 \geq 0.990$) describe the relation between the fat globule size and the bulk scattering properties of a milk sample. Therefore, inversion of the Mie solution could allow for the accurate estimation of the size distribution from measured bulk scattering properties. As this would enable the prediction of microstructure-related quality parameters, next to the compositional analysis used nowadays, this would considerably increase the value of Vis/NIR spectroscopy for agriculture and food industry. However, before this approach can be executed on very turbid suspensions like pure milk, further research is required to develop a model that describes dependent scattering in such media. Additionally, more research is needed with respect to the inversion of the Mie scattering model in order to enable fast, accurate and robust prediction of the particle size from bulk scattering properties.

Finally, it was found that casein micelles only have a limited contribution to the Vis/NIR bulk scattering properties of milk. Nevertheless, better understanding of the scattering by casein micelles would further improve the model that related the fat globule size with the Vis/NIR bulk scattering properties of the milk sample.

Acknowledgements

Ben Aernouts was funded as Ph. D. fellow of the Research Foundation-Flanders (FWO, grant 11A4813N). Rodrigo Watté, Robbe Van Beers, Tjebbe Huybrechts and Jeroen Jordens are funded by the Institute for the Promotion of Innovation through Science and Technology in Flanders (IWT-Flanders, respectively grants 101552, 131777, 121611 and 121235). The authors gratefully acknowledge IWT-Flanders for the financial support through the GlucoSens and Koesensor projects (respectively grants SB-090053 and LA-110770).

References and links

[1] G. Phillips, P. Williams, Handbook of Hydrocolloids, 2nd ed., WoodHead Publishing, Cambridge, UK, 2009.
[2] A. Parker, C. Baravian, F. Caton, J. Dillet, J. Mougel, Fast optical sizing without dilution, Food Hydrocoll. 21 (2007) 831–837.
[3] N. Argov, D.G. Lemay, J.B. German, Milk fat globule structure and function: nanoscience comes to milk production, Trends Food Sci. Technol. 19 (2008) 617–623.
[4] H.W. Heid, T.W. Keenan, Intracellular origin and secretion of milk fat globules, Eur. J. Cell Biol. 84 (2005) 245–258.
[5] P. Walstra, J. Wouters, T. Geurts, Dairy Science and Technology, 2nd ed., Taylor & Francis Group, Boca Raton, USA, 2006.
[6] G. Cabassi, M. Profaizer, L. Marinoni, N. Rizzi, T. Cattaneo, Estimation of fat globule size distribution in milk using an inverse light scattering model in the near infrared region, J. Near Infrared Spectrosc. 21 (2013) 359–373.
[7] P. Schenkel, R. Samudrala, J. Hinrichs, Thermo-physical properties of semi-hard cheese made with different fat fractions: Influence of melting point and fat globule size, Int. Dairy J. 30 (2013) 79–87.
[8] M.-C. Michalski, B. Camier, V. Briard, N. Leconte, J.-Y. Gassi, H. Goudédranche, et al., The size of native milk fat globules affects physico-chemical and functional properties of Emmental cheese, Lait. 84 (2004) 343–358.
[9] M.-C. Michalski, J.-Y. Gassi, M.-H. Famelart, N. Leconte, B. Camier, F. Michel, et al., The size of native milk fat globules affects physico-chemical and sensory properties of Camembert cheese, Lait. 83 (2003) 131–143.
[10] C. Garcia, C. Antona, B. Robert, C. Lopez, M. Armand, The size and interfacial composition of milk fat globules are key factors controlling triglycerides bioavailability in simulated human gastro-duodenal digestion, Food Hydrocoll. 35 (2014) 494–504.
[11] A. Berton, S. Rouvellac, B. Robert, F. Rousseau, C. Lopez, I. Crenon, Effect of the size and interface composition of milk fat globules on their in vitro digestion by the human pancreatic lipase: Native versus homogenized milk fat globules, Food Hydrocoll. 29 (2012) 123–134.
[12] S. Gallier, K.C. Gordon, R. Jiménez-Flores, D.W. Everett, Composition of bovine milk fat globules by confocal Raman microscopy, Int. Dairy J. 21 (2011) 402–412.

[13] C. Lopez, V. Briard-Bion, O. Ménard, E. Beaucher, F. Rousseau, J. Fauquant, et al., Fat globules selected from whole milk according to their size: Different compositions and structure of the biomembrane, revealing sphingomyelin-rich domains, Food Chem. 125 (2011) 355–368.
[14] S. Couvreur, C. Hurtaud, P.G. Marnet, P. Faverdin, J.L. Peyraud, Composition of milk fat from cows selected for milk fat globule size and offered either fresh pasture or a corn silage-based diet, J. Dairy Sci. 90 (2007) 392–403.
[15] C. Fauquant, V. Briard, N. Leconte, M.-C. Michalski, Differently sized native milk fat globules separated by microfiltration: fatty acid composition of the milk fat globule membrane and triglyceride core, Eur. J. Lipid Sci. Technol. 107 (2005) 80–86.
[16] M.-C. Michalski, V. Briard, P. Juaneda, CLA profile in native fat globules of different sizes selected from raw milk, Int. Dairy J. 15 (2005) 1089–1094.
[17] L. Wiking, J. Stagsted, L. Björck, J.H. Nielsen, Milk fat globule size is affected by fat production in dairy cows, Int. Dairy J. 14 (2004) 909–913.
[18] V. Briard, N. Leconte, F. Michel, M.-C. Michalski, The fatty acid composition of small and large naturally occurring milk fat globules, Eur. J. Lipid Sci. Technol. 105 (2003) 677–682.
[19] Y. Ma, D.M. Barbano, Gravity separation of raw bovine milk: fat globule size distribution and fat content of milk fractions., J. Dairy Sci. 83 (2000) 1719–1727.
[20] M.C. Michalski, N. Leconte, V. Briard-Bion, J. Fauquant, J.L. Maubois, H. Goudédranche, Microfiltration of raw whole milk to select fractions with different fat globule size distributions: process optimization and analysis, J. Dairy Sci. 89 (2006) 3778–3790.
[21] J. a O'Mahony, M. a E. Auty, P.L.H. McSweeney, The manufacture of miniature Cheddar-type cheeses from milks with different fat globule size distributions, J. Dairy Res. 72 (2005) 338–348.
[22] H. Timmen, S. Patton, Milk fat globules: fatty acid composition, size and in vivo regulation of fat liquidity, Lipids. 23 (1988) 685–689.
[23] A. Bogomolov, A. Melenteva, D. Dahm, Technical note: Fat globule size effect on visible and shortwave near infrared spectra of milk, J. Near Infrared Spectrosc. 21 (2013) 435–440.
[24] A. Bogomolov, A. Melenteva, Scatter-based quantitative spectroscopic analysis of milk fat and total protein in the region 400–1100nm in the presence of fat globule size variability, Chemom. Intell. Lab. Syst. 126 (2013) 129–139.
[25] D. Dahm, Review: Explaining some light scattering properties of milk using representative layer theory, J. Near Infrared Spectrosc. 21 (2013) 323–339.
[26] A. Bogomolov, S. Dietrich, B. Boldrini, R.W. Kessler, Quantitative determination of fat and total protein in milk based on visible light scatter, Food Chem. 134 (2012) 412–418.
[27] B. Aernouts, E. Polshin, W. Saeys, J. Lammertyn, Mid-infrared spectrometry of milk for dairy metabolomics: a comparison of two sampling techniques and effect of homogenization, Anal. Chim. Acta. 705 (2011) 88–97.
[28] M. Thiebaud, E. Dumay, L. Picart, J.P. Guiraud, J.C. Cheftel, High-pressure homogenisation of raw bovine milk. Effects on fat globule size distribution and microbial inactivation, Int. Dairy J. 13 (2003) 427–439.
[29] A. Logan, M. Auldist, J. Greenwood, L. Day, Natural variation of bovine milk fat globule size within a herd, J. Dairy Sci. 97 (2014) 4072–4082.
[30] N.I. Nielsen, T. Larsen, M. Bjerring, K.L. Ingvartsen, Quarter health, milking interval, and sampling time during milking affect the concentration of milk constituents, J. Dairy Sci. 88 (2005) 3186–3200.
[31] F. Vangroenweghe, H. Dosogne, C. Burvenich, Composition and milk cell characteristics in quarter milk fractions of dairy cows with low cell count, Vet. J. 164 (2002) 254–260.
[32] B. Aernouts, E. Polshin, J. Lammertyn, W. Saeys, Visible and near-infrared spectroscopic analysis of raw milk for cow health monitoring: reflectance or transmittance?, J. Dairy Sci. 94 (2011) 5315–5329.
[33] G. Katz, O. Shapira, L. Lemberskiy-Kuzin, N. Pinsky, System and method for on-line analysis and sorting of milk coagulation properties, US8072596, 2011.
[34] K. Mizuno, M. Hatsuno, K. Aikawa, H. Takeichi, T. Himi, A. Kaneko, et al., Mastitis is associated with IL-6 levels and milk fat globule size in breast milk, J. Hum. Lact. 28 (2012) 529–534.
[35] R.E. Erwin, H.E. Randolph, Influence of mastitis on properties of milk. XI. Fat globule membrane, J. Dairy Sci. 58 (1975) 9–12.
[36] A. Melfsen, E. Hartung, A. Haeussermann, Robustness of near-infrared calibration models for the prediction of milk constituents during the milking process., J. Dairy R. 80 (2013) 103–112.
[37] J.R. Frisvad, N.J. Christensen, H.W. Jensen, Computing the scattering properties of participating media using Lorenz-Mie theory, ACM Trans. Graph. 26 (2007) 60.
[38] C. Erkinbaev, E. Herremans, N. Nguyen Do Trong, E. Jakubczyk, P. Verboven, B. Nicolaï, et al., Contactless and non-destructive differentiation of microstructures of sugar foams by hyperspectral scatter imaging, Innov. Food Sci. Emerg. Technol. 24 (2014) 131–137.
[39] A. Torricelli, L. Spinelli, M. Vanoli, M. Leitner, A. Nemeth, N.D.T. Nguyen, et al., Optical Coherence Tomography (OCT), Space-resolved Reflectance Spectroscopy (SRS) and Time-resolved Reflectance Spectroscopy (TRS): Principles and Applications to Food Microstructures, in: V. Morris, K. Groves (Eds.), Food Microstruct. Microsc. Meas. Model., 1st ed., WoodHead Publishing, Cambridge, UK, 2013: p. 480.
[40] B. Aernouts, R. Watté, J. Lammertyn, W. Saeys, Modelling the effect of the fat globule size distribution on the scattering properties of milk, in: Proc. NIR2013, La Grande-Motte, France, 2013.
[41] R. Watté, N.D.T. Nguyen, B. Aernouts, C. Erkinbaev, J. De Baerdemaeker, B.M. Nicolaï, et al., Metamodeling approach for efficient estimation of optical properties of turbid media from spatially resolved diffuse reflectance measurements, Opt. Express. 21 (2013) 32630–32642.

[42] E. Herremans, E. Bongaers, P. Estrade, E. Gondek, M. Hertog, E. Jakubczyk, et al., Microstructure-texture relationships of aerated sugar gels: Novel measurement techniques for analysis and control, Innov. Food Sci. Emerg. Technol. 18 (2013) 202–211.
[43] V. V. Tuchin, Tissue Optics: Light Scattering Methods and Instruments for Medical Diagnosis, 2nd ed., SPIE Press, Washington, USA, 2007.
[44] K. Kaniyamattam, A. De Vries, Agreement between milk fat, protein, and lactose observations collected from the Dairy Herd Improvement Association (DHIA) and a real-time milk analyzer, J. Dairy Sci. 97 (2014) 2896–2908.
[45] B. Aernouts, R. Watté, R. Van Beers, F. Delport, M. Merchiers, J. De Block, et al., A flexible tool for simulating the bulk optical properties of polydisperse spherical particles in an absorbing host medium: a validation, Opt. Express. 22 (2014) 20223–20238.
[46] P. Bascom, R. Cobbold, On a fractal packing approach for understanding ultrasonic backscattering from blood, J. Acoust. Soc. Am. 98 (1995) 3040–3049.
[47] N. Berger, R. Lucas, V. Twersky, Polydisperse scattering theory and comparisons with data for red blood cells, J. Acoust. Soc. Am. 89 (1991) 1394–1401.
[48] B. Aernouts, R. Van Beers, R. Watté, J. Lammertyn, W. Saeys, Dependent scattering in intralipid phantoms in the 600-1850 nm range, Opt. Express. 22 (2014) 6086–6098.
[49] Z. Gaygadzhiev, M. Corredig, M. Alexander, Diffusing wave spectroscopy study of the colloidal interactions occurring between casein micelles and emulsion droplets: comparison to hard-sphere behavior, Langmuir. 24 (2008) 3794–3800.
[50] M. Alexander, L.F. Rojas-Ochoa, M. Leser, P. Schurtenberger, Structure, dynamics, and optical properties of concentrated milk suspensions: an analogy to hard-sphere liquids., J. Colloid Interface Sci. 253 (2002) 35–46.
[51] P. Fox, P. McSweeney, Advanced Dairy Chemistry, Volume 1: Proteins, 3rd ed., Kluwer Academic/Plenum Publishers, New York, USA, 2003.
[52] C. McCrae, A. Lepoetre, Characterization of dairy emulsions by forward lobe laser light scattering—Application to milk and cream, Int. Dairy J. 6 (1996) 247–256.
[53] M.-C. Michalski, M. Ollivon, V. Briard, N. Leconte, C. Lopez, Native fat globules of different sizes selected from raw milk: thermal and structural behavior, Chem. Phys. Lipids. 132 (2004) 247–261.
[54] M.-C. Michalski, F. Michel, D. Sainmont, V. Briard, Apparent ζ-potential as a tool to assess mechanical damages to the milk fat globule membrane, Colloids Surfaces B Biointerfaces. 23 (2002) 23–30.
[55] M.C. Michalski, V. Briard, F. Michel, F. Tasson, P. Poulain, Size distribution of fat globules in human colostrum, breast milk, and infant formula, J. Dairy Sci. 88 (2005) 1927–1940.
[56] M.-C. Michalski, F. Michel, C. Geneste, Appearance of submicronic particles in the milk fat globule size distribution upon mechanical treatments, Lait. 82 (2002) 193–208.
[57] M.-C. Michalski, V. Briard, F. Michel, Optical parameters of milk fat globules for laser light scattering measurements, Lait. 81 (2001) 787–796.
[58] M.C. Michalski, R. Cariou, F. Michel, C. Garnier, Native vs. damaged milk fat globules: membrane properties affect the viscoelasticity of milk gels, J. Dairy Sci. 85 (2002) 2451–2461.
[59] R. Attaie, R.L. Richter, Size distribution of fat globules in goat milk, J. Dairy Sci. 83 (2000) 940–944.
[60] C.L. Lopez, Focus on the supramolecular structure of milk fat in dairy products, Reprod. Nutr. Dev. 45 (2005) 497–511.
[61] O. Ménard, S. Ahmad, F. Rousseau, V. Briard-Bion, F. Gaucheron, C. Lopez, Buffalo vs. cow milk fat globules: Size distribution, zeta-potential, compositions in total fatty acids and in polar lipids from the milk fat globule membrane, Food Chem. 120 (2010) 544–551.
[62] A. Ye, S. Singh, H, Taylor, M., Anema, Disruption of fat globules during concentration of whole milk in a pilot scale multiple- effect evaporator, Int. J. Dairy Technol. 58 (2005) 143–149.
[63] a. Zamora, V. Ferragut, B. Guamis, a. J. Trujillo, Changes in the surface protein of the fat globules during ultra-high pressure homogenisation and conventional treatments of milk, Food Hydrocoll. 29 (2012) 135–143.
[64] a Zamora, V. Ferragut, P.D. Jaramillo, B. Guamis, a J. Trujillo, Effects of ultra-high pressure homogenization on the cheese-making properties of milk, J. Dairy Sci. 90 (2007) 13–23.
[65] C.M. Beliciu, C.I. Moraru, Effect of solvent and temperature on the size distribution of casein micelles measured by dynamic light scattering., J. Dairy Sci. 92 (2009) 1829–1839.
[66] C.G.K. de Kruif, T. Huppertz, Casein micelles: size distribution in milks from individual cows, J. Agric. Food Chem. 60 (2012) 4649–4655.
[67] C.G. de Kruif, Supra-aggregates of Casein Micelles as a Prelude to Coagulation, J. Dairy Sci. 81 (1998) 3019–3028.
[68] R. Gebhardt, W. Doster, J. Friedrich, U. Kulozik, Size distribution of pressure-decomposed casein micelles studied by dynamic light scattering and AFM., Eur. Biophys. J. 35 (2006) 503–509.
[69] M. Glantz, T.G. Devold, G.E. Vegarud, H. Lindmark Månsson, H. Stålhammar, M. Paulsson, Importance of casein micelle size and milk composition for milk gelation, J. Dairy Sci. 93 (2010) 1444–1451.
[70] M. Glantz, A. Håkansson, H. Lindmark Månsson, M. Paulsson, L. Nilsson, Revealing the size, conformation, and shape of casein micelles and aggregates with asymmetrical flow field-flow fractionation and multiangle light scattering, Langmuir. 26 (2010) 12585–12591.
[71] T. Huppertz, S. Grosman, P.F. Fox, A.L. Kelly, Heat and ethanol stabilities of high-pressure-treated bovine milk, Int. Dairy J. 14 (2004) 125–133.
[72] H. Mootse, A. Pisponen, S. Pajumägi, A. Polikarpus, V. Tatar, A. Sats, et al., Investigation of casein micelle particle size distribution in raw milk of Estonian holstein dairy cows, Agron. Res. 12 (2014) 753–758.

[73] M. Alexander, D.G. Dalgleish, Dynamic Light Scattering Techniques and Their Applications in Food Science, Food Biophys. 1 (2006) 2–13.
[74] T. Tran Le, P. Saveyn, H.D. Hoa, P. Van der Meeren, Determination of heat-induced effects on the particle size distribution of casein micelles by dynamic light scattering and nanoparticle tracking analysis, Int. Dairy J. 18 (2008) 1090–1096.
[75] J. Kuntsche, K. Klaus, F. Steiniger, Size determinations of colloidal fat emulsions: a comparative study, J. Biomed. Nanotechnol. 5 (2009) 384–395.
[76] S. Meyer, S. Berrut, T.I.J. Goodenough, V.S. Rajendram, V.J. Pinfield, M.J.W. Povey, A comparative study of ultrasound and laser light diffraction techniques for particle size determination in dairy beverages, Meas. Sci. Technol. 17 (2006) 289–297.
[77] S. V. Crowley, B. Desautel, I. Gazi, A.L. Kelly, T. Huppertz, J. a. O'Mahony, Rehydration characteristics of milk protein concentrate powders, J. Food Eng. 149 (2015) 105–113.
[78] E. de Kort, M. Minor, T. Snoeren, T. van Hooijdonk, E. van der Linden, Effect of calcium chelators on physical changes in casein micelles in concentrated micellar casein solutions, Int. Dairy J. 21 (2011) 907–913.
[79] S. Ji, M. Corredig, H.D. Goff, Aggregation of casein micelles and κ-carrageenan in reconstituted skim milk, Food Hydrocoll. 22 (2008) 56–64.
[80] A. Madadlou, M.E. Mousavi, Z. Emam-djomeh, M. Ehsani, D. Sheehan, Sonodisruption of re-assembled casein micelles at different pH values, Ultrason. Sonochem. 16 (2009) 644–648.
[81] A. Madadlou, M.E. Mousavi, Z. Emam-Djomeh, M. Ehsani, D. Sheehan, Comparison of pH-dependent sonodisruption of re-assembled casein micelles by 35 and 130kHz ultrasounds, J. Food Eng. 95 (2009) 505–509.
[82] A. Madadlou, M.E. Mousavi, Z. Emam-Djomeh, D. Sheehan, M. Ehsani, Alkaline pH does not disrupt re-assembled casein micelles, Food Chem. 116 (2009) 929–932.
[83] A. Mimouni, H.C. Deeth, A.K. Whittaker, M.J. Gidley, B.R. Bhandari, Rehydration process of milk protein concentrate powder monitored by static light scattering, Food Hydrocoll. 23 (2009) 1958–1965.
[84] S. Ahmad, I. Gaucher, F. Rousseau, E. Beaucher, M. Piot, J.F. Grongnet, et al., Effects of acidification on physico-chemical characteristics of buffalo milk: A comparison with cow's milk, Food Chem. 106 (2008) 11–17.
[85] H. Saveyn, T. Le Thu, R. Govoreanu, P. Van der Meeren, P. a. Vanrolleghem, In-line Comparison of Particle Sizing by Static Light Scattering, Time-of-Transition, and Dynamic Image Analysis, Part. Part. Syst. Charact. 23 (2006) 145–153.
[86] P. Walstra, On the stability of casein micelles, J. Dairy Sci. 73 (1990) 1965–1979.
[87] P. Walstra, R. Jenness, Dairy Chemistry and Physics, John Wiley and Sons, New York, USA, 1984.
[88] B. Aernouts, E. Zamora-Rojas, R. Van Beers, R. Watté, L. Wang, M. Tsuta, et al., Supercontinuum laser based optical characterization of turbid media in the 500-2250 nm range, Opt. Express. 21 (2013) 32450–32467.
[89] S.A. Prahl, Everything I think you should know about inverse adding-doubling, Http://omlc.ogi.edu/software/iad/iad-3-9-10.zip. (2010).
[90] G.M. Hale, M.R. Querry, Optical constants of water in the 200-nm to 200-μm wavelength region, Appl. Opt. 12 (1973) 555–563.
[91] S. Sharma, M. Goodarzi, H. Ramon, W. Saeys, Performance evaluation of preprocessing techniques utilizing expert information in multivariate calibration., Talanta. 121 (2014) 105–112.
[92] E. Zamora-Rojas, B. Aernouts, A. Garrido-Varo, D. Pérez-Marín, J.E. Guerrero-Ginel, W. Saeys, Double integrating sphere measurements for estimating optical properties of pig subcutaneous adipose tissue, Innov. Food Sci. Emerg. Technol. 19 (2013) 218–226.
[93] S. Jacquemoud, S. Ustin, J. Verdebout, G. Schmunck, G. Andreoli, B. Hosgood, Estimating leaf biochemistry using the PROSPECT leaf optical properties model, Remote Sens. Environ. 56 (1996) 194–202.
[94] S.J. Lee, J.W. Sherbon, Chemical changes in bovine milk fat globule membrane caused by heat treatment and homogenization of whole milk, J. Dairy Res. 69 (2002) 555–567.
[95] P. Di Ninni, F. Martelli, G. Zaccanti, Effect of dependent scattering on the optical properties of Intralipid tissue phantoms, Biomed. Opt. Express. 2 (2011) 2265–2278.
[96] A. Giusto, R. Saija, M.A. Iatì, P. Denti, F. Borghese, O.I. Sindoni, Optical properties of high-density dispersions of particles: application to intralipid solutions, Appl. Opt. 42 (2003) 4375–4380.
[97] A. Ishimaru, Y. Kuga, Attenuation constant of a coherent field in a dense distribution of particles, J. Opt. Soc. Am. 72 (1982) 1317–1320.
[98] J.M. Schmitt, G. Kumar, Optical scattering properties of soft tissue: a discrete particle model, Appl. Opt. 37 (1998) 2788–2797.
[99] G. Zaccanti, S. Del Bianco, F. Martelli, Measurements of optical properties of high-density media, Appl. Opt. 42 (2003) 4023–4030.
[100] D.W. Mackowski, M.I. Mishchenko, Direct simulation of extinction in a slab of spherical particles, J. Quant. Spectrosc. Radiat. Transf. 123 (2013) 103–112.
[101] M. Mishchenko, L. Liu, D. Mackowski, B. Cairns, G. Videen, Multiple scattering by random particulate media: exact 3D results, Opt. Express. 15 (2007) 2822–2836.
[102] D.W. Mackowski, M.I. Mishchenko, Calculation of the T matrix and the scattering matrix for ensembles of spheres, J. Opt. Soc. Am. A. 13 (1996) 2266–2278.
[103] V.D. Nguyen, D.J. Faber, E. Van Der Pol, T.G. Van Leeuwen, J. Kalkman, Dependent and multiple scattering in transmission and backscattering optical coherence tomography, Opt. Express. 21 (2013) 29145–29156.
[104] M.I. Mishchenko, D.H. Goldstein, J. Chowdhary, A. Lompado, Radiative transfer theory verified by controlled laboratory experiments, Opt. Lett. 38 (2013) 3522–3525.

[105] L. Wang, X. Sun, F. Li, Generalized eikonal approximation for fast retrieval of particle size distribution in spectral extinction technique, Appl. Opt. 51 (2012) 2997–3005.

Figures

Fig. 1 The cumulative volume-frequency particle size distributions for the raw and homogenized milk samples.

Fig. 2 The cumulative volume-frequency particle size distributions for the raw and homogenized milk samples after subtraction of the casein contribution. The casein fraction itself is also illustrated.

Fig. 3 Microscopic images (1250x magnification) of fat globules in raw milk. The black scale bar in the bottom-right corner represents 10 µm.

Fig. 4 Microscopic images (1250x magnification) of fat globules in the raw milk sample (Fig. 3) after 120 s of ultrasonic homogenization. The black scale bar in the bottom-right corner represents 10 µm.

Fig. 5 Microscopic images (1250x magnification) of fat globules in the raw milk sample (Fig. 3) after 1200 s of ultrasonic homogenization. The black scale bar in the bottom-right corner represents 10 µm.

Fig. 6 Measured bulk absorption coefficient spectra (μ_a) for the undiluted raw and homogenized milk samples.

Fig. 7 Measured bulk scattering coefficient spectra (μ_s) for the undiluted raw and homogenized milk samples.

Fig. 8 Measured scattering anisotropy spectra (g) for the undiluted raw and homogenized milk samples.

Fig. 9 Bulk scattering coefficient μ_s for raw and homogenized (for 120 s and 1200 s) milk samples measured on pure samples ($^1/_1$) and two- ($^1/_2$) and three-fold dilutions ($^1/_3$) of the same sample. The μ_s spectra for the diluted samples ($^1/_2$ and $^1/_3$) are rescaled to the particle concentration of the pure sample through multiplication by respectively 2 and 3, following the linear independent scattering relation.

Fig. 10 Measured and simulated (*) bulk scattering coefficient spectra (μ_s) for three-fold diluted raw and homogenized milk samples. The simulated bulk scattering coefficient spectrum for the 'virtual' casein fraction is also illustrated.

Fig. 11 Measured and simulated (*) scattering anisotropy spectra (g) for three-fold diluted raw and homogenized milk samples. The simulated scattering anisotropy spectrum for the 'virtual' casein fraction is also illustrated.

Tables

Table 1 Most important properties of the volume-frequency particle size distributions for the raw (Raw), homogenized (* s) and skimmed (Skim) milk samples (Fig. 1 and Fig. 2) before (a) and after (b) subtraction of the casein micelle contribution. The properties of the casein micelle fraction (Casein) itself are also shown in (b). The Dv10, Dv50 and Dv90 are respectively the 10^{th}, 50^{th} and 90^{th} percentile of the volume-based particle size distribution. The D32 and D43 are respectively the Sauter and DeBroukere mean particle diameter.

53 Table 2 Coefficients of determination, indicating the agreement between measured and
54 simulated bulk optical properties for the raw and homogenized milk samples illustrated in Fig.
55 10 and Fig. 11.

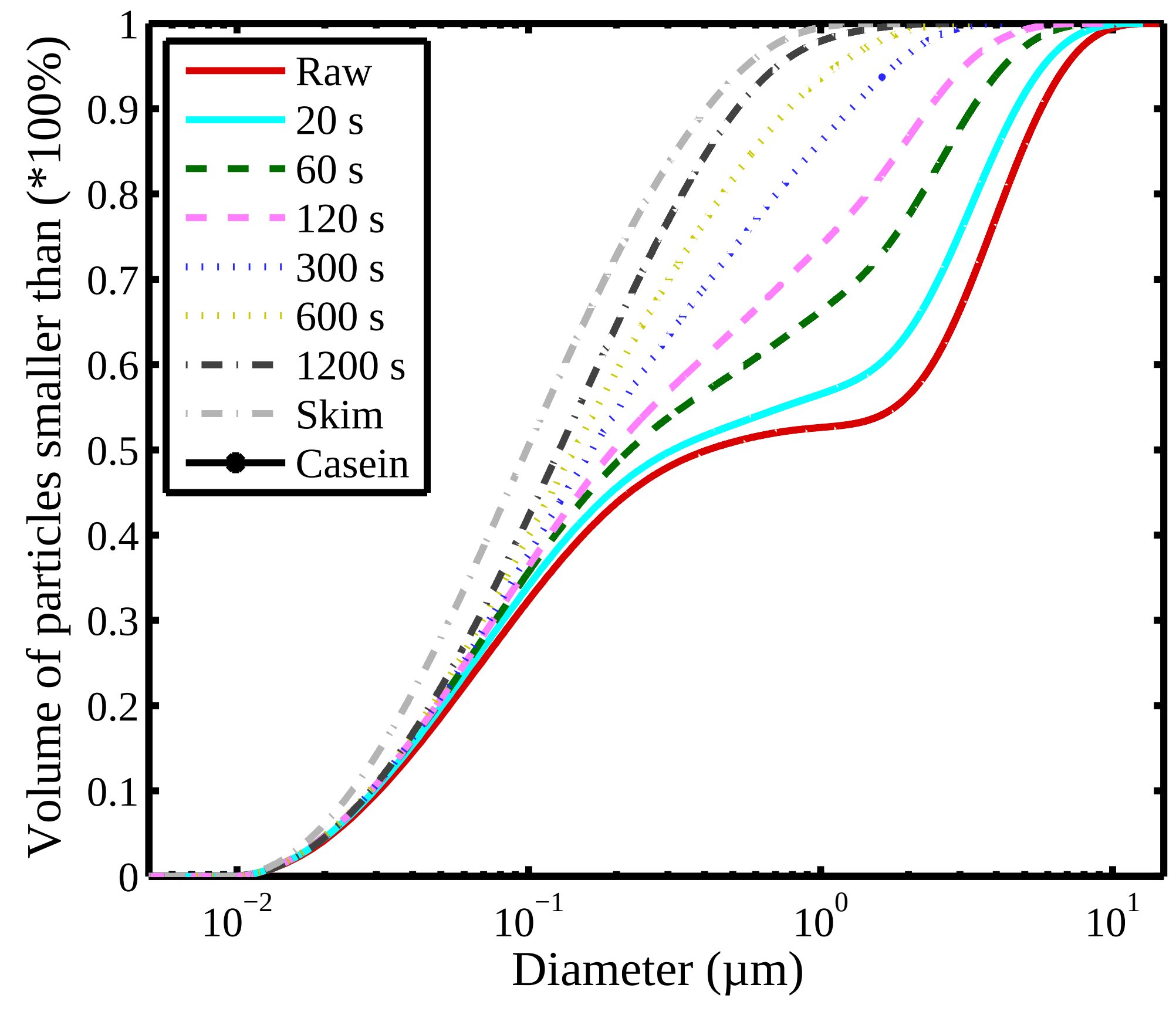
Raw
20 s
60 s
120 s
300 s
600 s
1200 s
Skim
Casein
Volume of particles smaller than (*100%)
Diameter (µm)
0
0.1
0.2
0.3
0.4
0.5
0.6
0.7
0.8
0.9
1
10^{-2}
10^{-1}
10^{0}
10^{1}

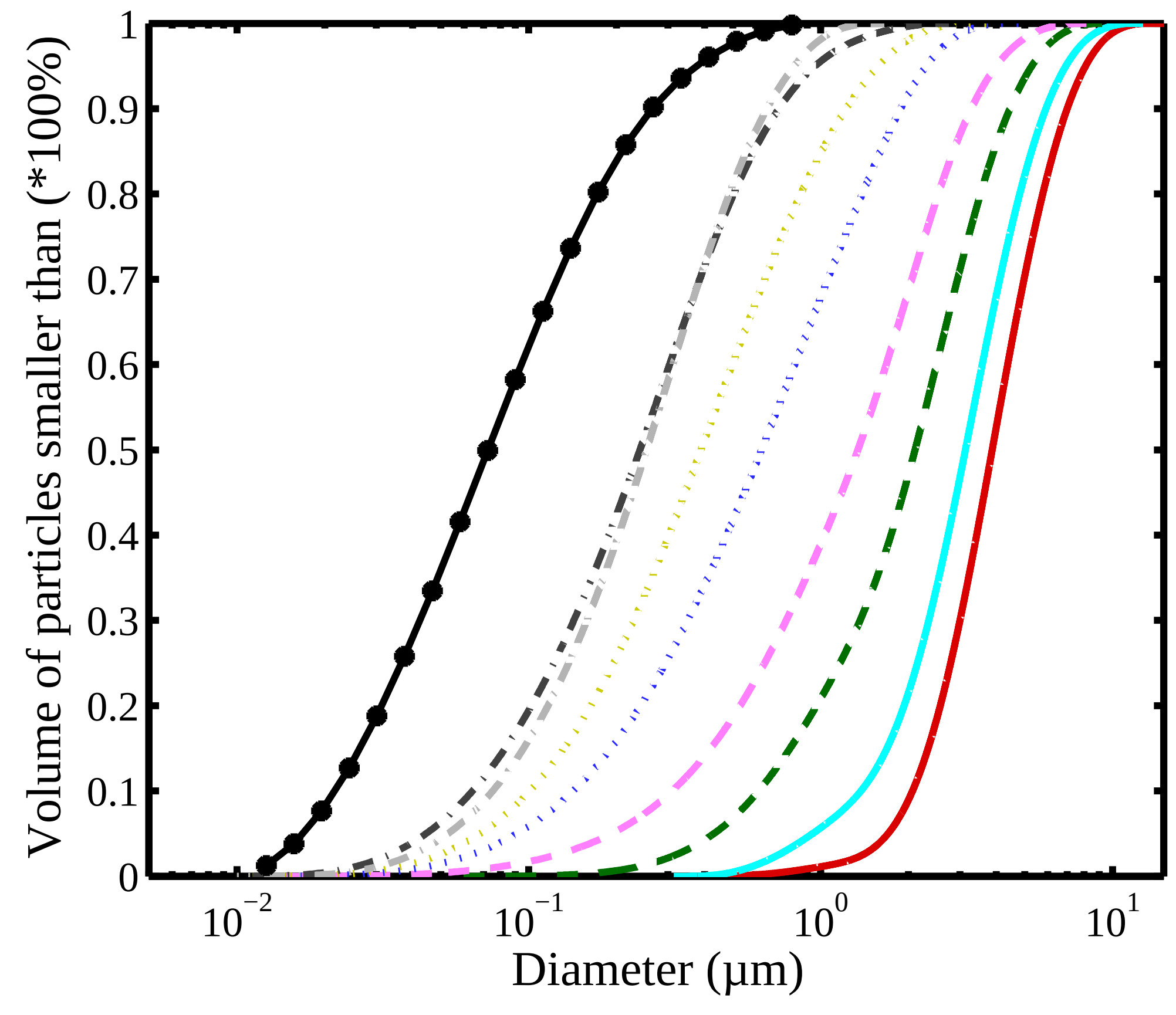
Volume of particles smaller than (*100%)
1
0.9
0.8
0.7
0.6
0.5
0.4
0.3
0.2
0.1
0
10^{-2}
10^{-1}
10^{0}
10^{1}
Diameter (µm)

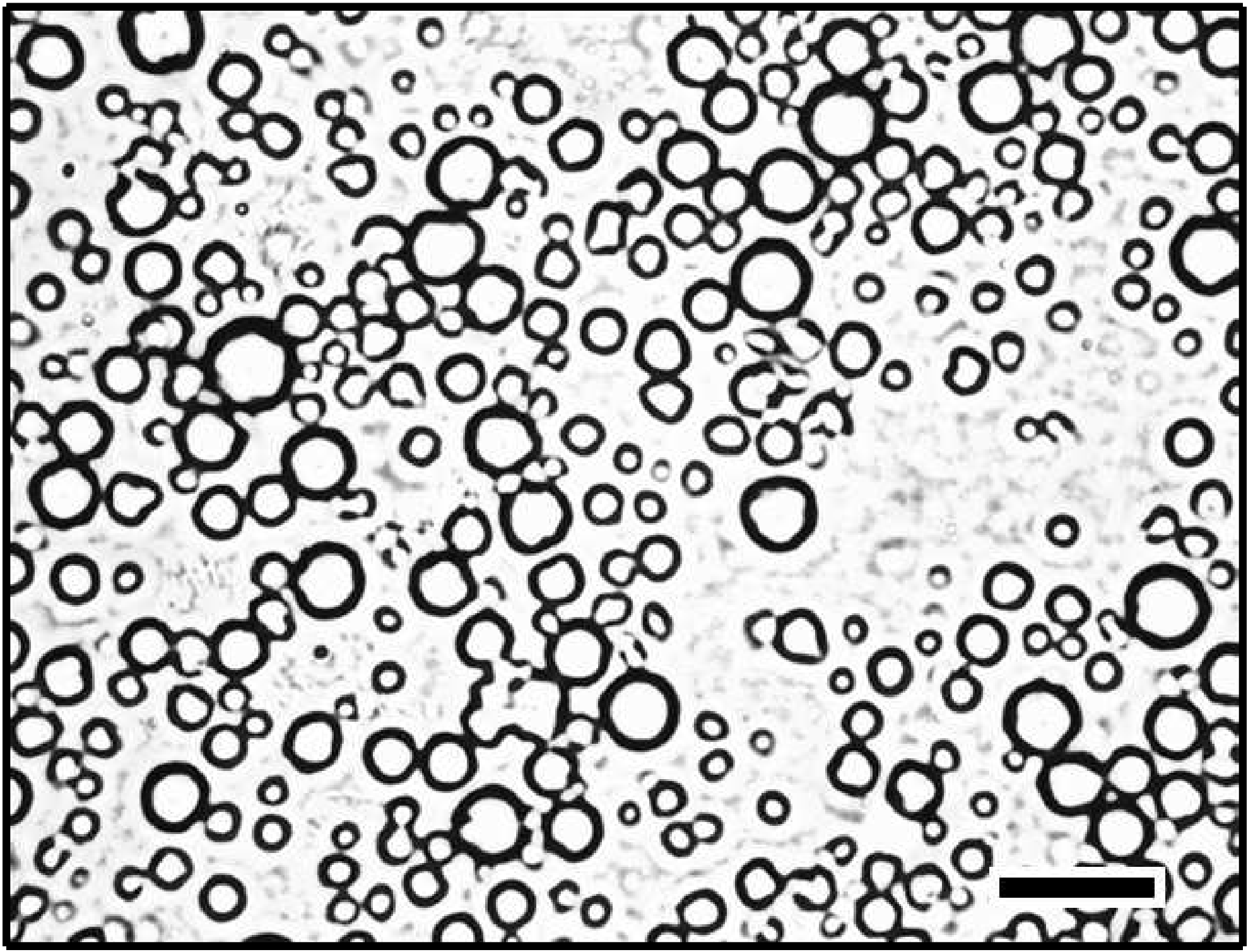

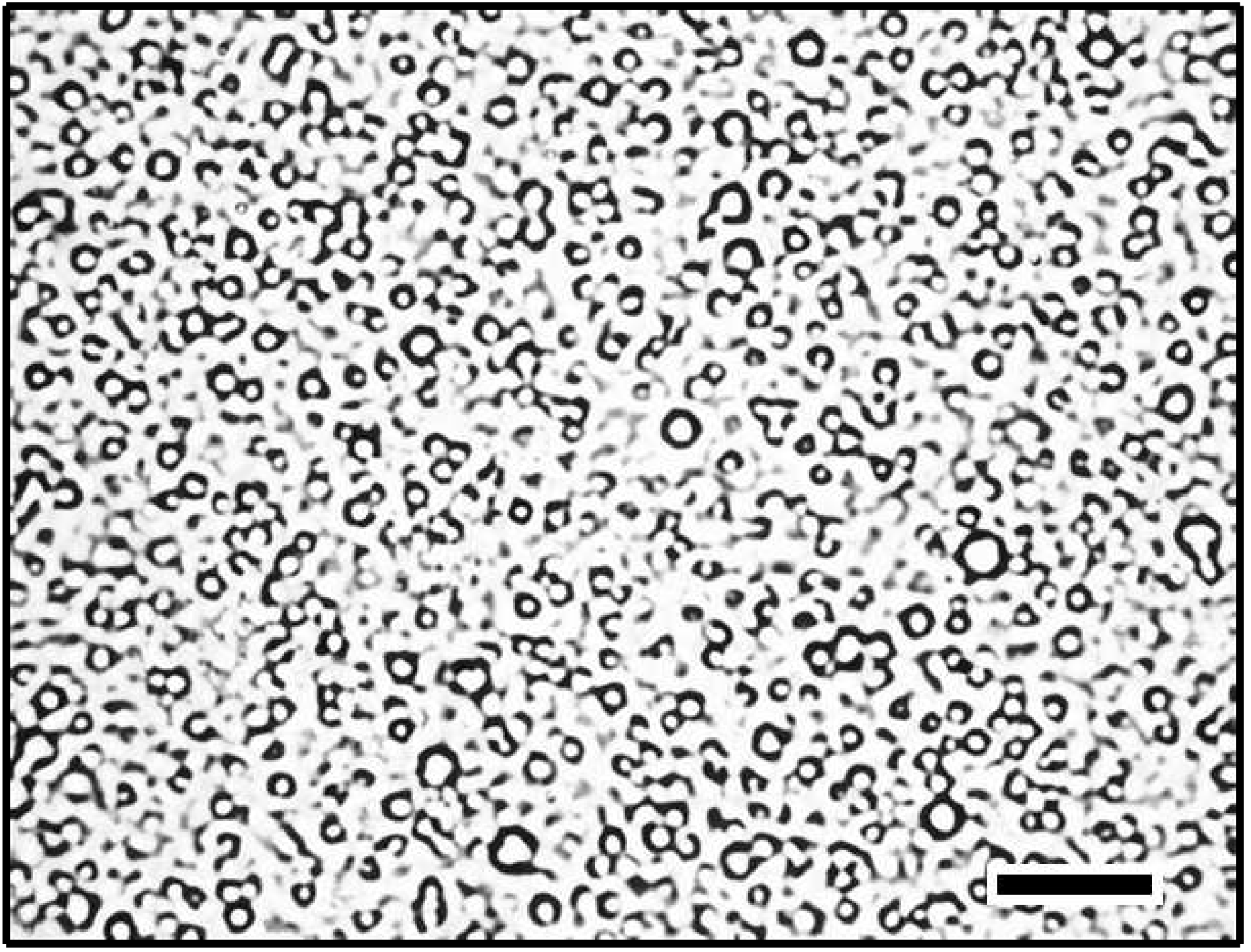

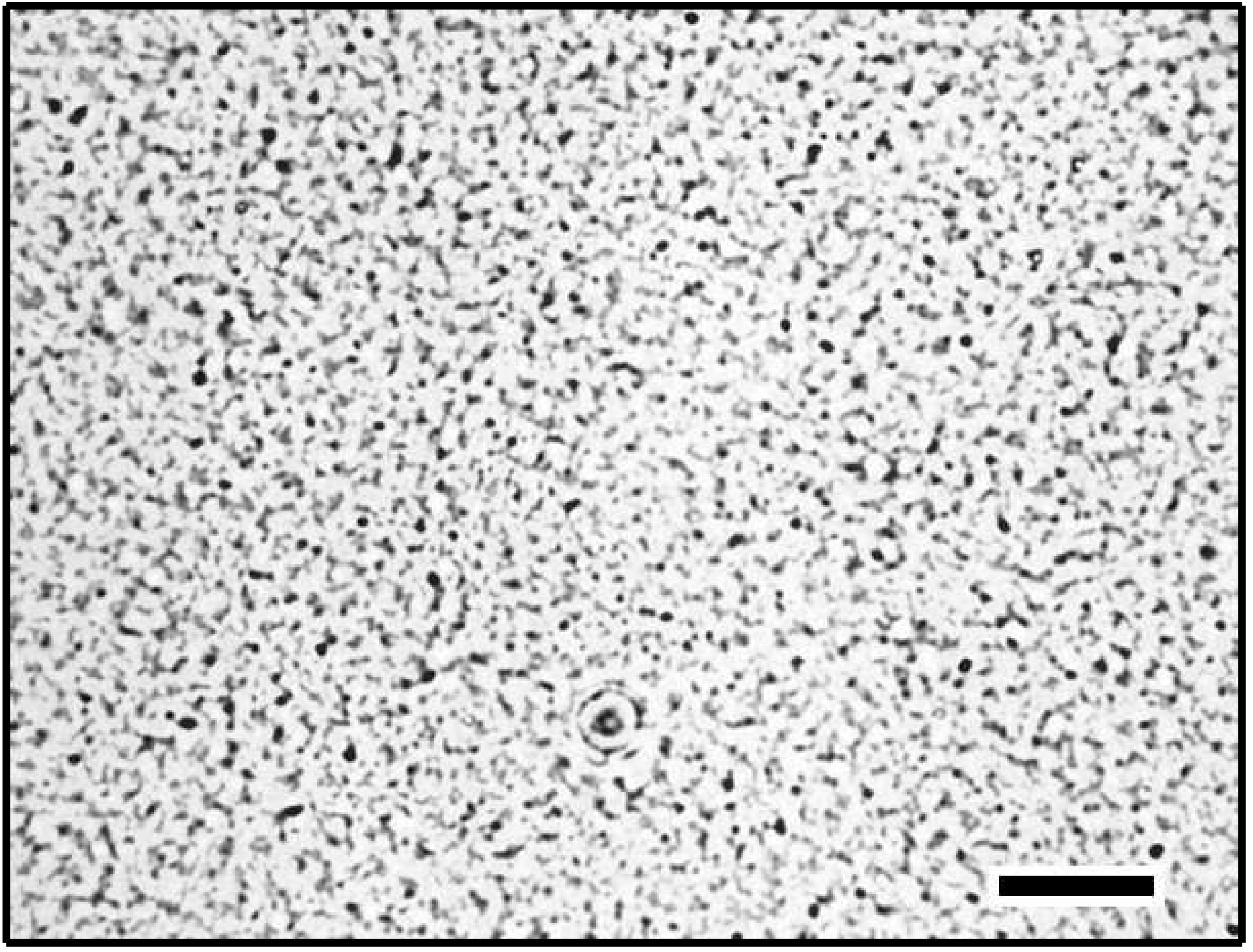

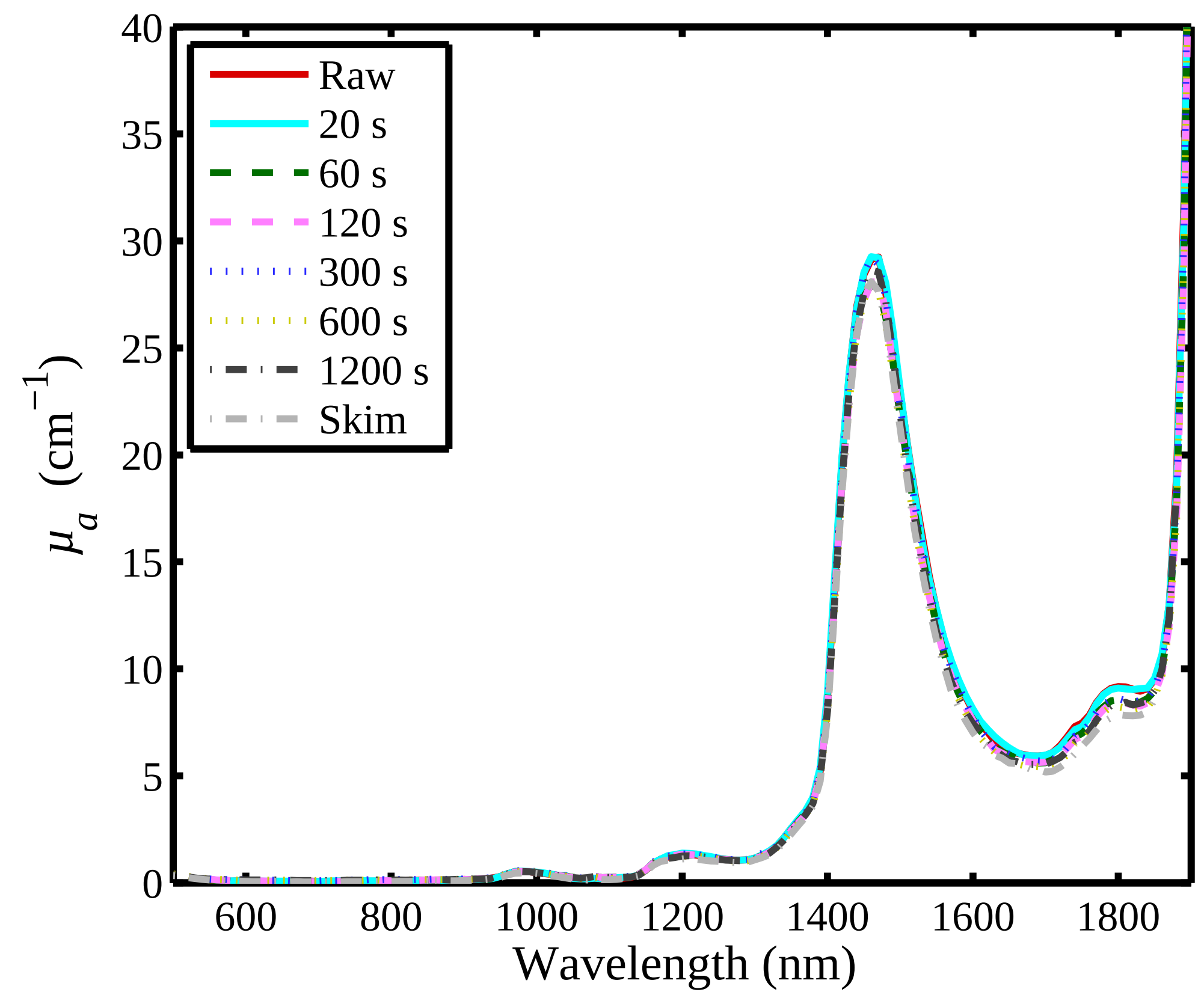
Raw
20 s
60 s
120 s
300 s
600 s
1200 s
Skim
μ_a (cm^{-1})
Wavelength (nm)
0
5
10
15
20
25
30
35
40
600
800
1000
1200
1400
1600
1800

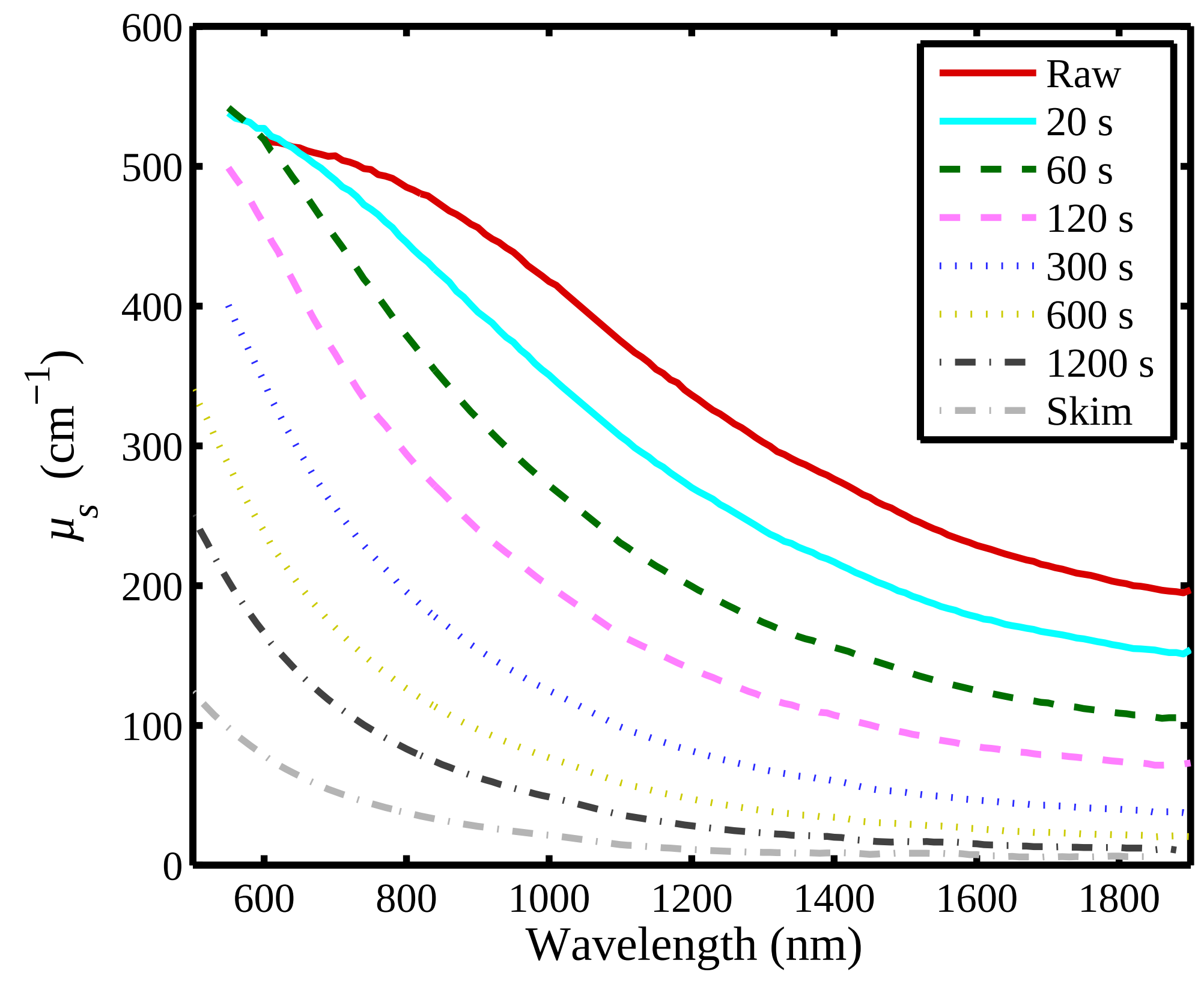
600
500
400
300
200
100
0
μ_s (cm^{-1})
600
800
1000
1200
1400
1600
1800
Wavelength (nm)
Raw
20 s
60 s
120 s
300 s
600 s
1200 s
Skim

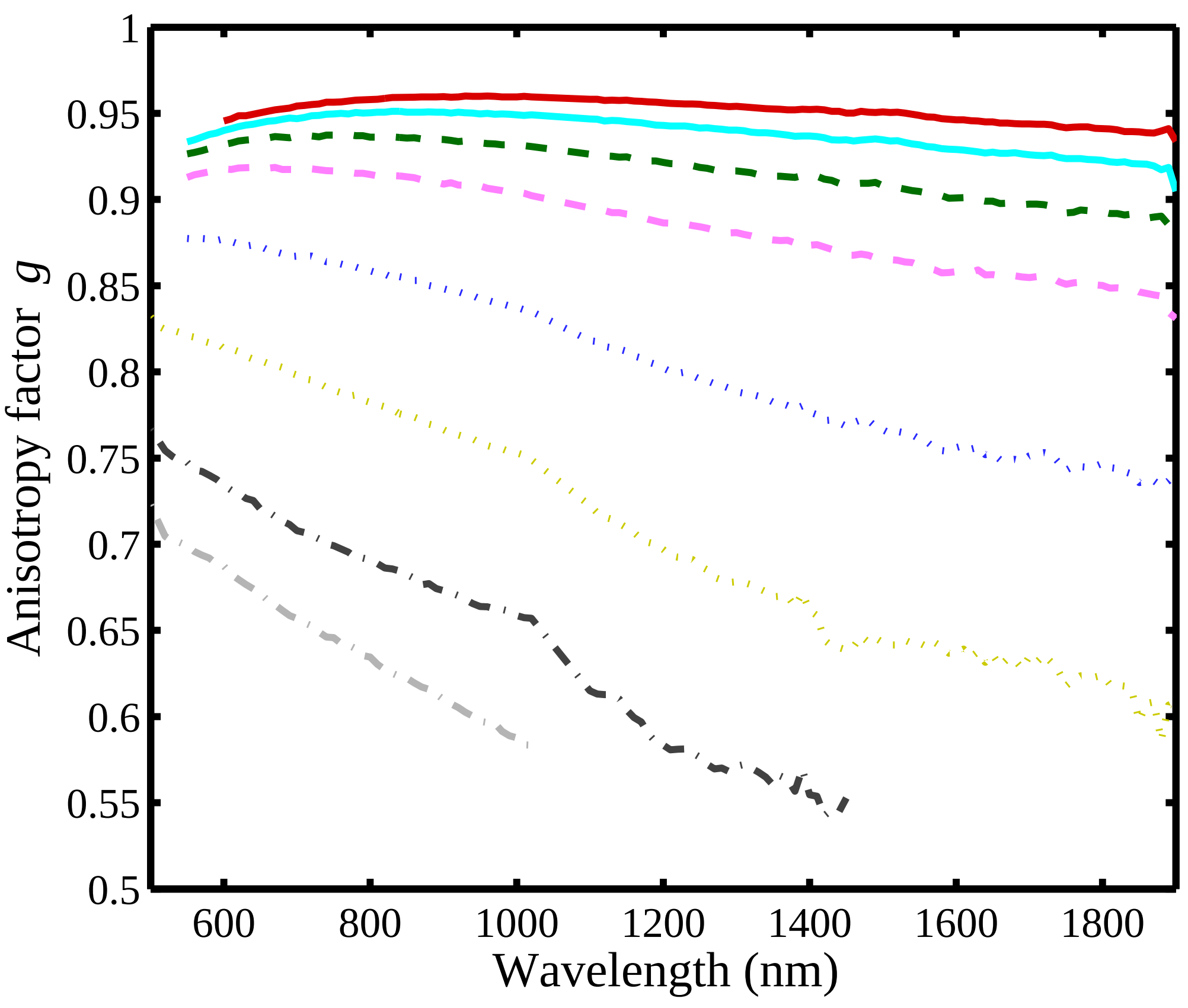
1
0.95
0.9
0.85
0.8
0.75
0.7
0.65
0.6
0.55
0.5
Anisotropy factor g
600
800
1000
1200
1400
1600
1800
Wavelength (nm)

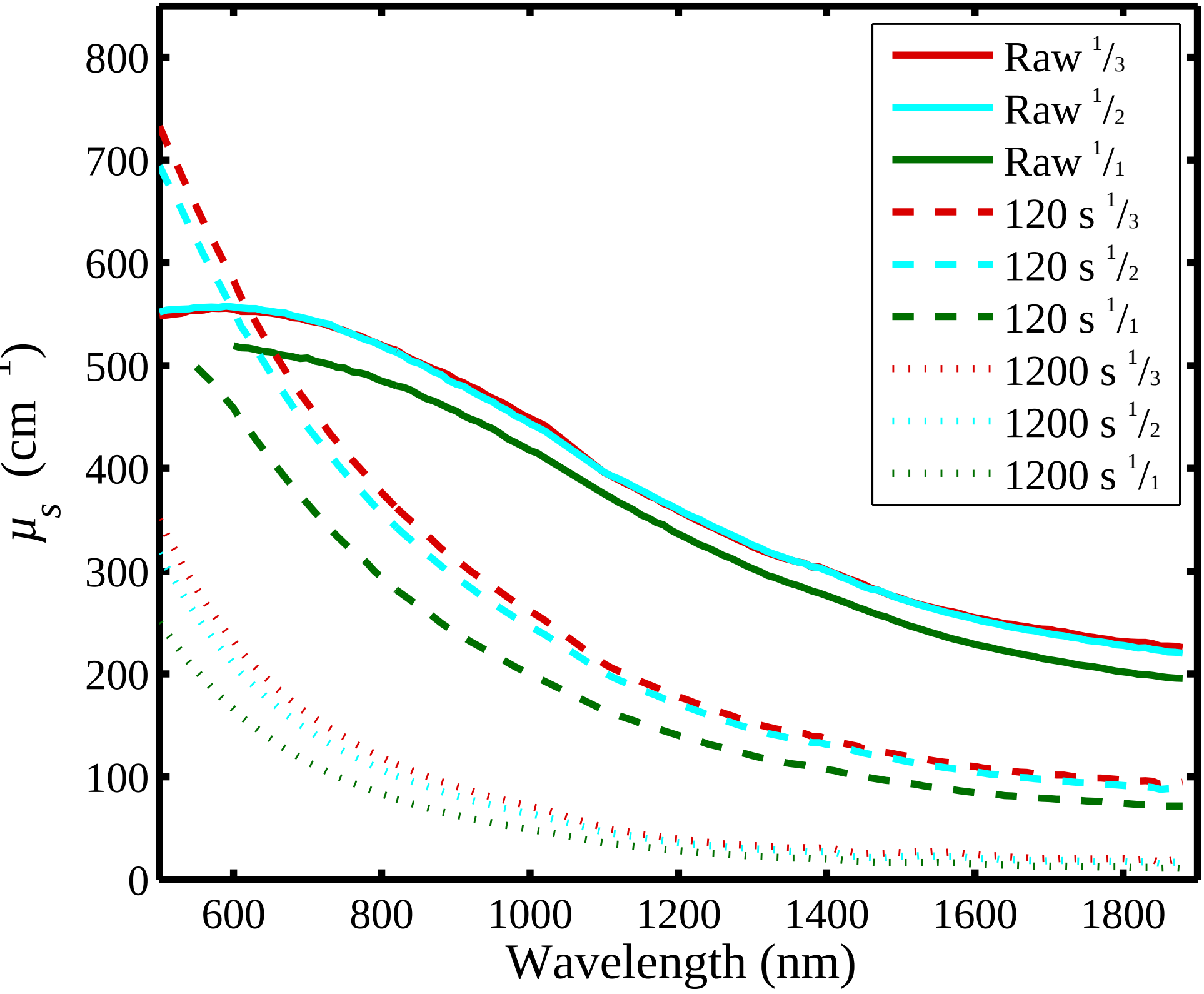
800
700
600
500
400
300
200
100
0
μ_s (cm^{-1})
600
800
1000
1200
1400
1600
1800
Wavelength (nm)
Raw 1/3
Raw 1/2
Raw 1/1
120 s 1/3
120 s 1/2
120 s 1/1
1200 s 1/3
1200 s 1/2
1200 s 1/1

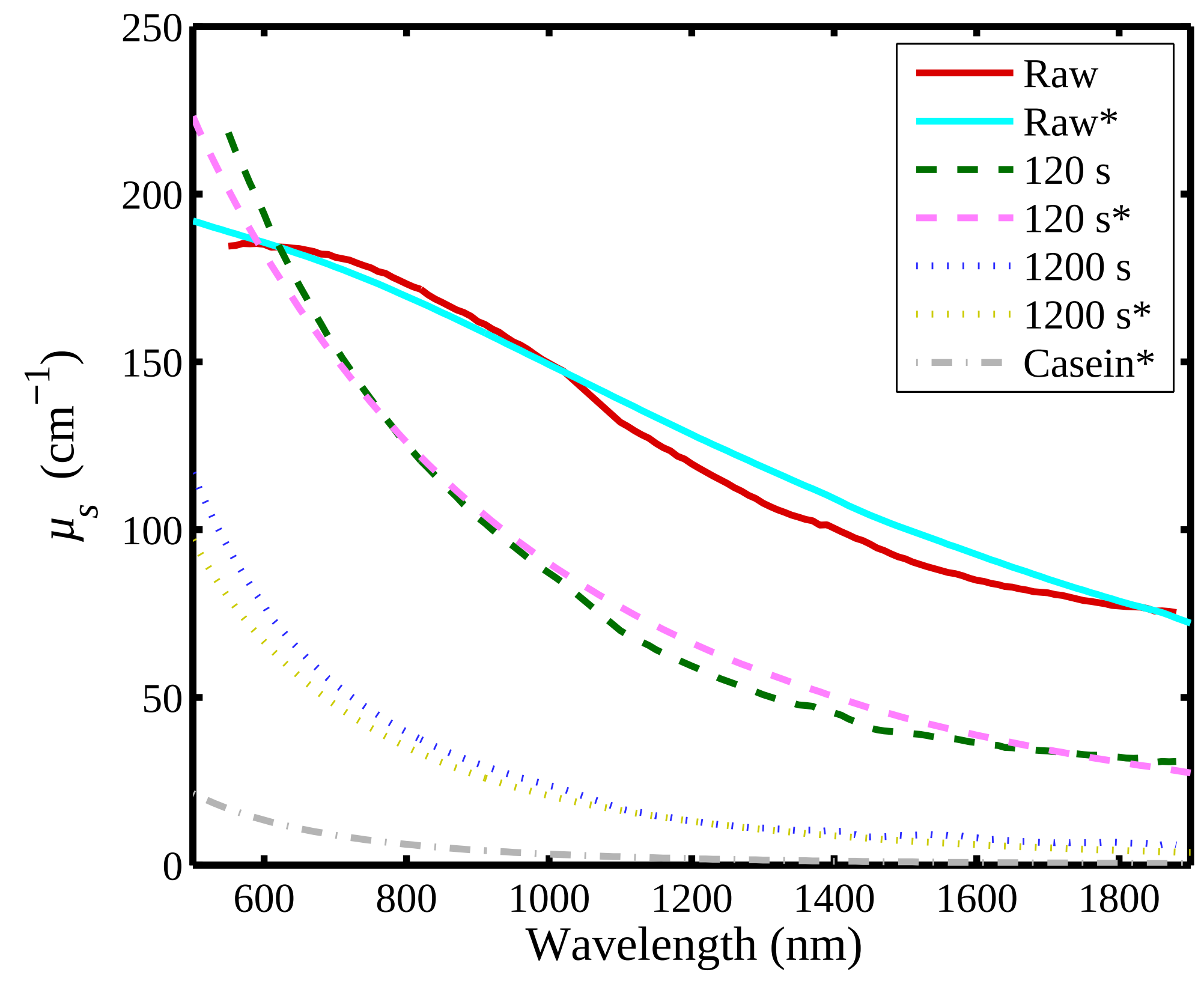
250
200
150
100
50
0
600
800
1000
1200
1400
1600
1800
Wavelength (nm)
μ_s (cm^{-1})
Raw
Raw*
120 s
120 s*
1200 s
1200 s*
Casein*

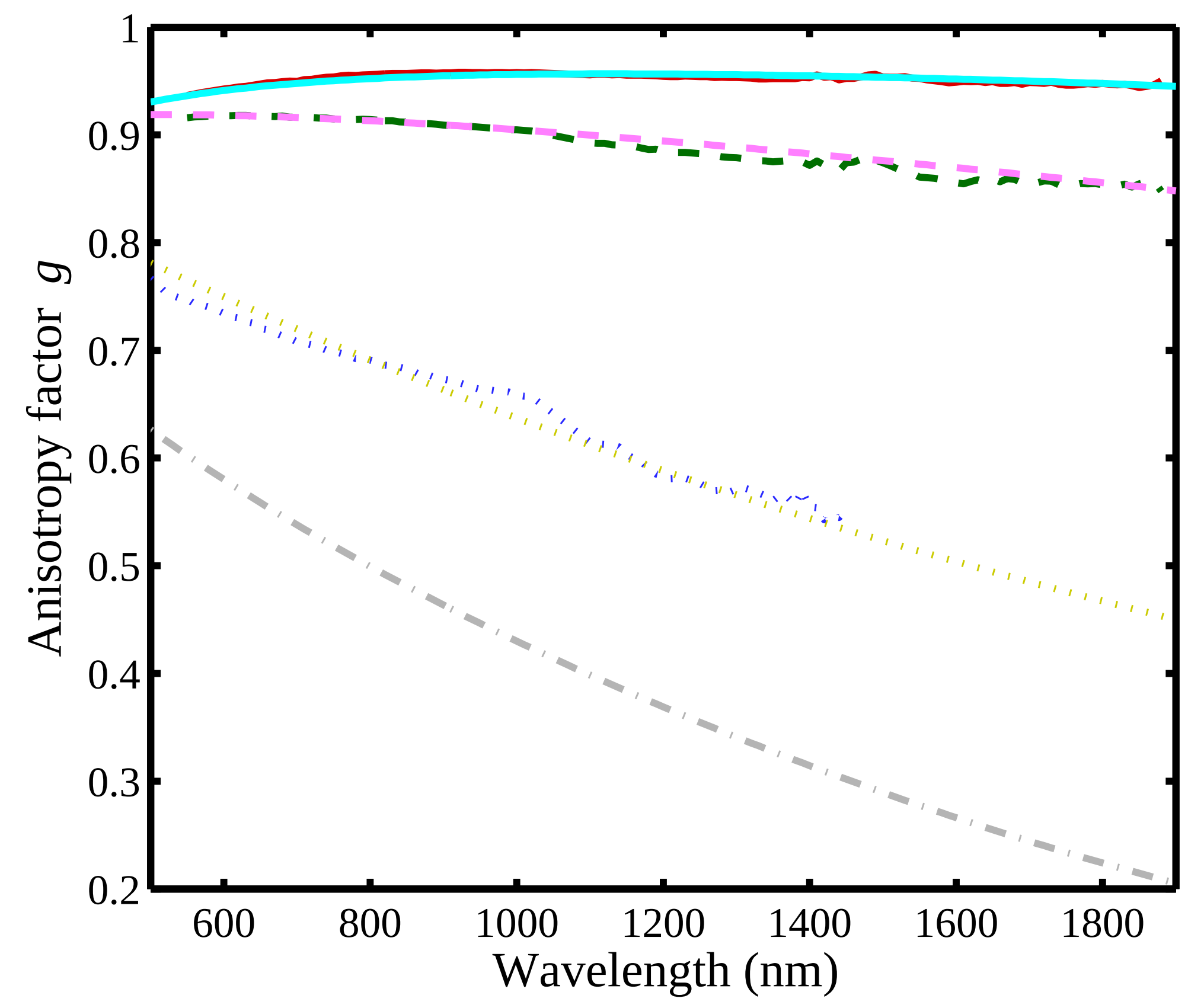
1
0.9
0.8
0.7
0.6
0.5
0.4
0.3
0.2
Anisotropy factor g
600
800
1000
1200
1400
1600
1800
Wavelength (nm)

Table 1 Most important properties of the volume-frequency particle size distributions for the raw (Raw), homogenized (* s) and skimmed (Skim) milk samples (Fig. 1 and Fig. 2) before (a) and after (b) subtraction of the casein micelle contribution. The properties of the casein micelle fraction (Casein) itself are also shown in (b). The Dv10, Dv50 and Dv90 are respectively the 10th, 50th and 90th percentile of the volume-based particle size distribution. The D32 and D43 are respectively the Sauter and DeBroukere mean particle diameter.

Sample	(a) With casein (μm)					(b) Casein subtraction (μm)				
	Dv10	Dv50	Dv90	D32	D43	Dv10	Dv50	Dv90	D32	D43
Raw	0.0306	0.411	5.69	0.0947	2.09	2.06	3.87	6.99	3.34	4.24
20 s	0.0295	0.312	4.67	0.0897	1.65	1.37	3.13	5.91	2.44	3.44
60 s	0.0288	0.222	3.30	0.0848	1.07	0.613	2.11	4.45	1.31	2.36
120 s	0.0288	0.195	2.35	0.0826	0.753	0.310	1.34	3.28	0.648	1.61
300 s	0.0288	0.165	1.27	0.0789	0.431	0.142	0.627	1.88	0.321	0.844
600 s	0.0285	0.143	0.777	0.0748	0.298	0.101	0.389	1.22	0.226	0.545
1200 s	0.0287	0.127	0.518	0.0721	0.219	0.0642	0.240	0.719	0.145	0.336
Skim	0.0248	0.0984	0.407	0.0606	0.167	0.0753	0.253	0.655	0.162	0.317
Casein						0.0217	0.0724	0.264	0.0501	0.116

Table 2 Coefficients of determination, indicating the agreement between measured and simulated bulk optical properties for the raw and homogenized milk samples illustrated in Fig. 10 and Fig. 11.

Sample	$R^2_{\mu_s}$	R^2_g
Raw	0.979	0.777
120 s	0.990	0.943
1200 s	0.954	0.964
Combined	**0.990**	**0.996**